

Chemical shift magnetic resonance imaging for distinguishing minimal-fat renal angiomyolipoma from renal cell carcinoma: a meta-analysis

Ling-Shan Chen¹ · Zheng-Qiu Zhu² · Zhi-Tao Wang¹ · Jing Li¹ · Li-Feng Liang¹ · Ji-Yang Jin³ · Zhong-Qiu Wang¹

Received: 23 June 2017 / Revised: 7 October 2017 / Accepted: 17 October 2017 / Published online: 24 November 2017
© European Society of Radiology 2017

Abstract

Objectives To determine the performance of chemical shift signal intensity index (CS-SII) values for distinguishing minimal-fat renal angiomyolipoma (mfAML) from renal cell carcinoma (RCC) and to assess RCC subtype characterisation.

Methods We identified eligible studies on CS magnetic resonance imaging (CS-MRI) of focal renal lesions via PubMed, Embase, and the Cochrane Library. CS-SII values were extracted by lesion type and evaluated using linear mixed model-based meta-regression. RCC subtypes were analysed. Two-sided p value <0.05 indicated statistical significance. Methodological quality was assessed using the Quality Assessment of Diagnostic Accuracy Studies 2 tool.

Results Eleven articles involving 850 patients were included. Minimal-fat AML had significantly higher CS-SII value than RCC ($p < 0.05$); there were no significant differences between mfAML and clear cell RCC (cc-RCC) ($p = 0.112$). Clear cell RCC had a significantly higher CS-SII value than papillary RCC (p-RCC) ($p < 0.001$) and chromophobe RCC (ch-RCC) ($p = 0.045$). The methodological quality was relatively high, and Begg's test data points indicated no obvious publication bias.

Conclusions The CS-SII value for differentiating mfAML from cc-RCC remains unproven, but is a promising method for differentiating cc-RCC from p-RCC and ch-RCC.

Key Points

- RCC CS-SII values are significantly lower than those of mfAML overall.
- CS-SII values cannot aid differentiation between mfAML and cc-RCC.
- CS-SII values might help characterise RCC subtypes.

Keywords Renal cell carcinoma · Minimal-fat angiomyolipoma · Chemical shift magnetic resonance imaging · Chemical shift signal intensity index · Differentiation

Introduction

Angiomyolipoma (AML), the most common benign renal tumour, is histologically composed of various proportions of adipose tissue, smooth muscle, and thick-walled blood vessels [1]. Originally, evidence of macroscopic fat within a renal cortical tumour on computed tomography (CT) or magnetic resonance imaging (MRI) was considered a unique, identifying feature of classic AML [2–4]. However, macroscopic fat may be subtle or completely absent in minimal-fat AML (mfAML), which account for approximately 5% of AML [5]. Meanwhile, there are extensive findings that some renal cell carcinomas (RCC) can contain either some macroscopic fat or minimal fat content owing to lipid-producing tumour necrosis, bone metaplasia with fatty marrow elements, or perinephric or renal sinus fat entrapment [6, 7]. Moreover, clear cell RCC (cc-RCC) frequently contain varying amounts of intracellular lipid and glycogen in addition to macroscopic fat [8, 9]. Consequently, these overlapping imaging features may lead to the misinterpretation of mfAML as RCC, and lead to some patients undergoing unnecessary surgery.

✉ Zhong-Qiu Wang
Zhq2001us@163.com

¹ Department of Radiology, Affiliated Hospital of Nanjing University of Chinese Medicine, Nanjing 210029, China

² Department of Ultrasound, Affiliated Hospital of Nanjing University of Chinese Medicine, Nanjing 210029, China

³ Department of Radiology, Zhongda Hospital of Southeast University, Nanjing 210029, China

Chemical shift MRI (CS-MRI), which has been widely used for differentiating adrenal adenoma from other neoplasms by quantifying the minimal fat content [10–12], is a useful technique for diagnosing mfAML [13, 14]. In CS-MRI, a decrease in signal intensity (SI) on opposed-phase gradient-echo images is a function of the ratio of lipid content to the total amount of tissue in each voxel. In general, a substantial CS SI index [CS-SII = $(SI_{in} - SI_{opp}) / (SI_{in}) \times 100$], where SI_{in} is the in-phase SI and SI_{opp} is the opposed-phase SI, decrease (CS-SII > 20–25%) appears indicative of either cc-RCC or AML [15, 16]. In mouse liver, Peng et al. [17] proved a strong correlation between liver fat content and CS-MRI ($r = 0.882$). Yet, no pathological or in vitro radiological research comparing the actual kidney lipid content between mfAML and cc-RCC has been performed so far, and the added value of in vivo evaluation of the small intratumoural lipid content by MRI using double-echo CS sequences is controversial. Some studies [18, 19] have reported that the CS-SII is a useful value for distinguishing mfAML from other renal neoplasms, whereas others [20–24] have observed a negative result.

Therefore, we aimed in this meta-analysis to review published studies that used the CS-SII value to differentiate mfAML and RCC to define the impact of this technique in routine practice for the characterisation of renal tumours and furthermore to assess its capability for classifying RCC subtypes.

Materials and methods

Literature search and selection

The PubMed, Cochrane Library and Embase databases were searched systematically for relevant published articles. The search strategy was based on the combination of the following keywords: (“MRI” OR “magnetic resonance imaging”) AND (“renal” OR “kidney”) AND (“neoplasm” OR “tumor” OR “cancer” OR “carcinoma” OR “lesion”). The inclusion criteria were: (1) CS-SII value was used to determine mfAML or primary malignancy of a renal lesion; (2) data were analysed on a per-lesion basis; (3) histopathological results and/or clinical follow-up were used as the reference standard; (4) absolute data of CS-SII values could be obtained. The article search was limited to those published in English. Review articles, letters, case reports and conference abstracts were excluded due to insufficient data.

Data extraction and quality assessment

Two investigators reviewed the included articles and extracted the relevant details independently for the meta-analysis, resolving any differences by consensus. The

extracted study characteristics were: first author, year of publication, country of origin, sample characteristics [number of patients and lesions, mean age, sex, study design, type of renal lesion, region of interest (ROI)], CS-SII parameters (modality, magnetic field strength, imaging sequences) and reference standard (Table 1). In addition, the absolute data of CS-SII values were recorded for further analysis. The Quality Assessment of Diagnostic Accuracy Studies 2 (QUADAS-2) tool [25] was used to extract the appropriate study design characteristics from each study, and consisted of 11 items: each was answered with “yes”, “no”, or “unknown”. “Yes” was assigned 1 score, and “no” or “unknown” was assigned 0 score. A score of 9 was used as a cut-off value for high versus low quality.

Statistical analysis

The CS-SII values of mfAML or RCC subtypes were extracted on a per-lesion basis. Based on these data, and regardless of the analysis population (intention to treat vs per protocol), meta-regression analyses based on a linear mixed model for pooled mean CS-SII values with 95% confidence intervals (CIs) was conducted using STATA software (ver. 12.0; StataCorp, College Station, TX, USA). Owing to the lack of information on the different analysis populations, we did not perform sensitivity analyses. We performed subgroup analyses on the RCC subtypes. In addition, publication bias was examined using Begg’s test. The level of statistical significance was set to a two-sided p value of 0.05.

Heterogeneity across studies was evaluated using Cochran’s Q -statistic ($p < 0.05$ was considered significant) and the I^2 test (0%, no heterogeneity; 100%, maximal heterogeneity). A random- or fixed-effects model was used based on the heterogeneity analysis. A random-effects model was used when there was significant heterogeneity among studies ($p < 0.05$ or $I^2 > 50%$); otherwise, a fixed-effects model was used. In either case, the results should be interpreted with care.

Results

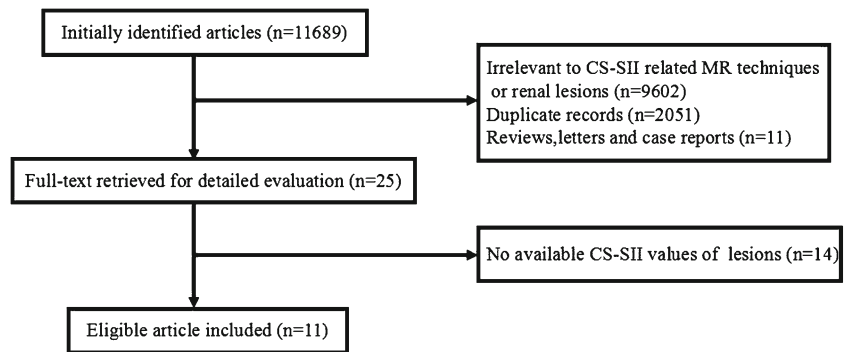
Literature search and study description

The search initially yielded 11,689 articles (deadline, 31 May 2017). Figure 1 shows the detailed flow chart of the literature search. Eventually, 11 articles involving 850 patients and 1,183 CS-SII measurements met the inclusion and exclusion criteria and were selected for data extraction and data analysis. There were a total 127 and 436 measurements for mfAML and RCC, respectively. RCC was divided into cc-RCC ($n = 427$), papillary RCC (p-RCC, $n = 156$), and chromophobe RCC (ch-RCC, $n = 37$). Table 1 lists the pooled characteristics of these 11 articles.

Table 1 Characteristics of studies included in the meta-analysis

Study	Year published	Country of origin	Patients (no.)	Mean age	Sex (M/F)	Study design	Lesions design (no.)	mfAML	RCC	cc-RCC	p-RCC	ch-RCC	Other RCC subtypes or neoplasms	ROI	CS-MRI parameters	Reference standard	QUADAS-2 score
Kim Sasiwimonphan	2006 2012	South Korea Thailand	55 111	49 ± 14 59.7	29/26 69/42	P R	55 119	26 15	NO 104	NO 62	NO 31	NO NO	29 NO	Centre of tumour Largest possible tumour area	Siemens 1.5-T dual-echo GRE GE 1.5-T or 3.0-T spoiled GRE	HP + CFU HP	7 10
Hindman	2012	United States	108	ND	65/43	R	108	20	NO	88	NO	NO	NO	Centre of tumour	Siemens 1.5-T or GE 1.5-T TIW GRE	HP	9
Cornelis Akita	2013 2013	France Japan	59 7	63 ND	35/24 7/0	R R	63 10	NO NO	43 NO	NO 5	NO 2	NO NO	20 3	Centre of tumour Largest possible tumour area	Philips 1.5-T TIW GRE GE 1.5-T TIW dual-echo GRE	HP HP	10 9
Cornelis Fere	2014 2014	France France	90 118	64.1 61	58/32 ND	R R	100 119	4 12	NO 95	57 54	16 32	7 7	16 12	ND Within the solid tumour component only	TIW GRE GEMS 1.5-T dual-echo GRE	HP HP	10 9
Schieda	2016	Canada	79	ND	40/39	R	87	10	NO	33	35	9	NO	Centre slice and encompassing up to two-thirds of the tumour	Siemens or GE 1.5-T or 3.0-T 2D or 3D TIW dual-echo GRE	HP	9
Hakim	2016	Canada	5	59.6	1/4	R	5	5	NO	NO	NO	NO	NO	Centre of tumour	Siemens 1.5-T or 3.0-T TIW GRE	HP	9
Jeong	2016	South Korea	168	ND	ND	R	173	18	155	116	20	16	3	Centre of tumour	Siemens or GE 1.5-T or Philips 3.0-T FSPGR 3D FFE	HP	9
Park	2017	South Korea	56	ND	ND	R	56	17	39	12	22	5	NO	Largest possible tumour area	Philips 3.0-T TIW dual-echo GRE	HP	10

ND not documented, NO no lesions included, mfAML minimal fat angiomyolipoma, RCC renal cell carcinoma, cc-RCC clear cell renal cell carcinoma, p-RCC papillary renal cell carcinoma, ch-RCC chromophobe renal cell carcinoma, ROI region of interest, HP histopathological results, CFU clinical follow-up, GRE gradient-recalled echo, TIW T1-weighted, FSPGR fast spoiled gradient-echo, FFE fast field echo

Fig. 1 Flow diagram of the study selection procedure

Quality assessment and publication bias

The quality assessment results in Table 1 demonstrate the QUADAS-2 questions for each study. There were overall high scores for the questions relating to quality of patient selection [91% (10/11 studies) to 100% (11/11 studies) of studies received a score for “yes”] and quality of index test interpretation [91% (10/11 studies) to 100% (11/11 studies)]. However, the scores for the question on the quality of reference standard interpretation were relatively lower [55% (6/11 studies)], largely related to the lack of exhibition in the literature four of the 11 studies (36%). The question on the interval between the index test and reference standard examination also had lower scores [18% (2/11 studies)], generally related to the inclusion of patients with an undocumented time interval between MRI and the reference standard examination. In summary, ten studies were high quality (score ≥ 9), and only one study was low quality (score = 7). In addition, Begg’s test found no significant publication bias (mfAML, $p = 0.175$; RCC, $p = 0.308$; cc-RCC, $p = 0.536$; ch-RCC, $p = 0.296$; p-RCC, $p = 0.566$).

Pooled estimates and subgroup analyses

Table 2 shows the pooled results, Figs. 2 and 3 show forest plots of the CS-SII values of mfAML, and RCC and its subtypes. The summarised CS-SII values for mfAML, RCC, and cc-RCC were 13.63 (95% CI, 10.15–17.12), 7.92 (95% CI, 4.78–11.07) and 9.99 (95% CI, 7.17–12.82), respectively. The CS-SII measurement of mfAML was significantly higher than that of RCC ($p = 0.017$), yet no significant differences were observed in the comparison between mfAML and cc-RCC ($p = 0.11$). For RCC subtype, the CS-SII measurement of cc-RCC was significantly higher than that of p-RCC [9.99 (95% CI, 7.17–12.82) vs -5.69 (95% CI, -8.40 to -2.98), $p < 0.001$] and ch-RCC [9.99 (95% CI, 7.17–12.82) vs 1.82 (95% CI, -5.68 to 9.32), $p = 0.045$]. However, the CS-SII values of p-RCC and ch-RCC were not significantly different ($p = 0.06$). This is illustrated in Fig. 4.

Discussion

Generally, the diagnosis of renal AML depends on the detection of intratumoural macroscopic fat on CT. Nevertheless, only 3–10% mature fat is microscopically detected in AML [26], in which fat is not visible on CT and is distributed heterogeneously [5, 27, 28]. New evidence [20, 29] shows that fat levels are substantially lower in the estimated percentage volume of intratumoural fat of surgical mfAML compared with surgically removed “classic” AML. In contrast, the presence of microscopic fat is non-specific and can also be seen in RCC, especially cc-RCC. Owing to the histological characteristic of dissolved lipids and cholesterol accumulation in the cytoplasm in cc-RCC [9, 30], abundant cytoplasmic lipid is observed in as many as 60% of cc-RCC [16]. Therefore, making a correct diagnosis for preoperative differentiation of mfAML and RCC, especially cc-RCC, is challenging.

CS-MRI (also known as in-phase and out-of-phase imaging, or opposed-phase imaging) has been proved extremely useful for characterising lesions and organs with fatty [12, 31–33] or lipid-poor [12, 34] components, and appears to be the most reliable method for differentiating adenomas from non-adenomas [34–36]. Recently, the CS-SII value has also been used to differentiate mfAML and other renal neoplasms. Outwater et al. [16] first used CS-MRI for identifying intracellular lipid within renal neoplasms, and suggested that both AML and cc-RCC exhibit a decreased SI on opposed-phase

Table 2 Number of cases and CS-SII values of renal lesion subtypes

Lesion	Number	Pooled CS-SII	SE	95% CI
mfAML	127	13.63	1.77	10.15–17.12
RCC	436	7.92	1.61	4.78–11.07
cc-RCC	427	9.99	1.44	7.17–12.82
P-RCC	156	-5.69	1.38	-8.40–2.98
ch-RCC	37	1.82	3.82	-5.68–9.32

CS-SII chemical shift signal intensity index, SE standard error, CI confidence interval, mfAML minimal fat angiomyolipoma, RCC renal cell carcinoma, cc-RCC clear cell renal cell carcinoma, p-RCC papillary renal cell carcinoma, ch-RCC chromophobe renal cell carcinoma

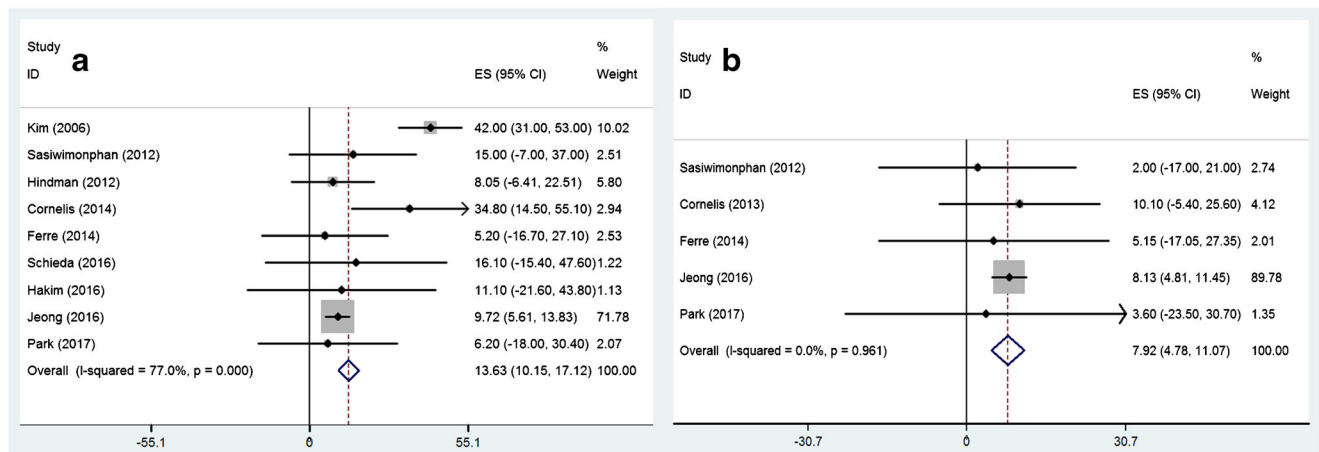


Fig. 2 Forest plots of CS-SII values for mfAML (a) and RCC (b)

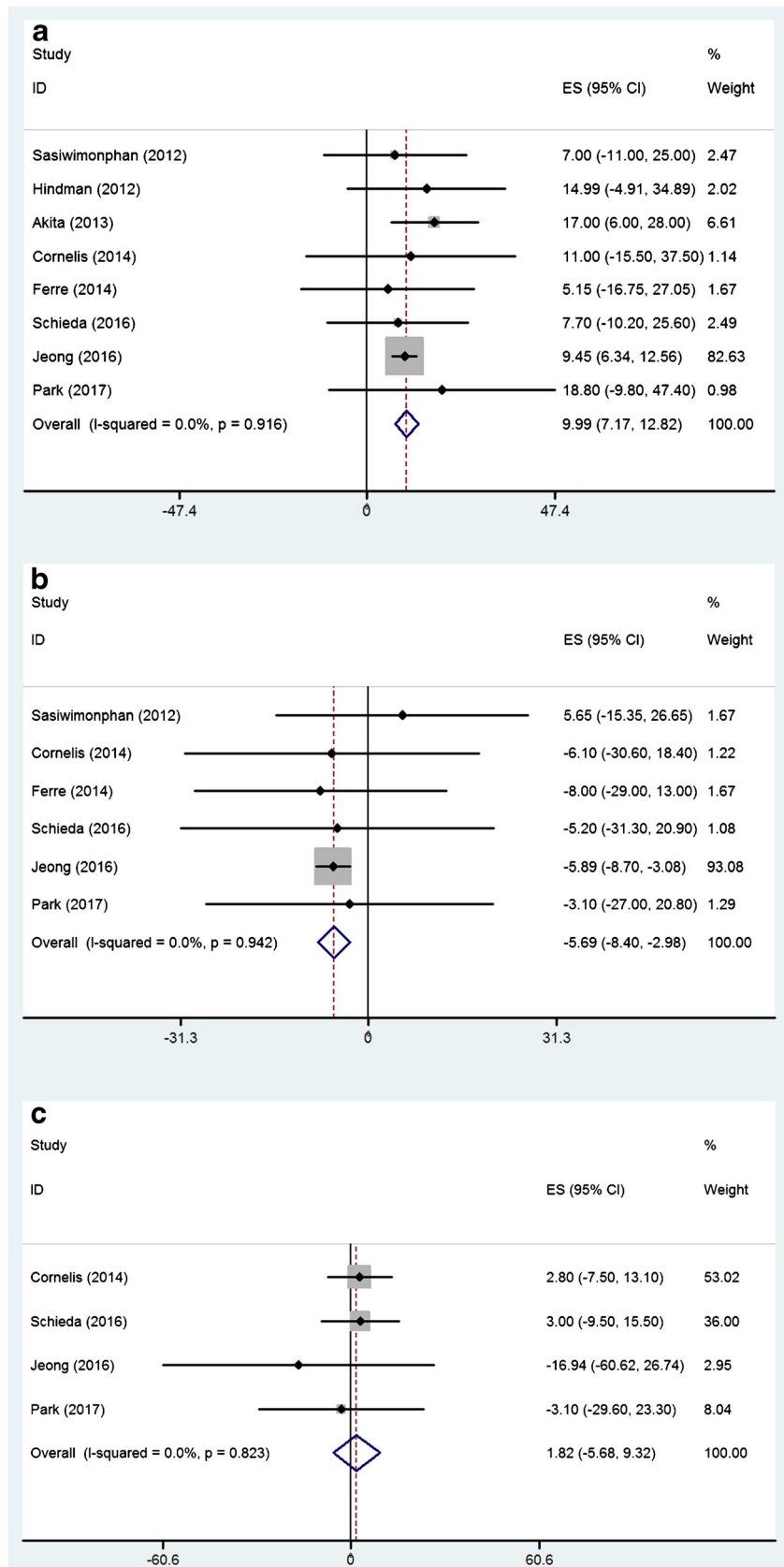
images. However, the value of CS-MRI for differentiating mfAML and RCC is controversial. Kim et al. [18] and Sasiwimonphan et al. [19] reported that SI loss on opposed-phase images of CS-MRI was higher for mfAML compared with cc-RCC. Nevertheless, Jhaveri et al. [24] confirmed a significantly higher percentage SI decrease in cc-RCC cases (median, 24.3%) than in either mfAML (median, 3.2%) or non-cc-RCC (median, -0.8%). Yet, other studies [20–23] have reported conflicting results, with no difference between the CS-SII values of mfAML and cc-RCC. The present meta-analysis pooled those estimates and showed that, overall, mfAML and cc-RCC exhibit a similar decrease in SI, reflecting a similar amount of intravoxel fat ($p = 0.11$) (Fig. 4). This means that CS-SII might not be a suitable MRI parameter for differentiating mfAML and cc-RCC, and may thereby lead to inaccurate diagnosis. However, the use of other multivariate analyses for MRI findings, and the combination of low T2-weighted imaging (T2WI) and/or apparent diffusion coefficient (ADC) signal is highly accurate for diagnosing mfAML, while cc-RCC always manifests as heterogeneously isointense to hyperintense to the renal cortex on T2WI and with moderate restricted diffusion [37]. The enhancement pattern, i.e. hyperenhancement during the corticomedullary phase of enhancement with gadolinium washout over time, overlapped between the two tumours [38]. Furthermore, the presence of intratumoural haemorrhage or calcification are highly specific for RCC and are not observed in mfAML [37].

Different RCC subtypes have unique histopathological features, genetic expression patterns and clinical behaviour [36, 39]. Previous studies have suggested that patients with p-RCC or ch-RCC have better prognosis than patients with cc-RCC [40, 41]. In addition, particularly in patients with advanced and metastatic RCC, these subtypes respond differently to molecular targeted therapies: the tyrosine kinase inhibitors sunitinib and sorafenib are more effective against cc-RCC, whereas temsirolimus has recently been shown to be more

effective against non-cc-RCC [42–44]. Therefore, accurate identification of the specific pathologic diagnosis prior to treatment is critical. Current multiparametric MRI, such as dynamic contrast enhancement (DCE) and diffusion-weighted imaging (DWI), might be a valid diagnostic approach for characterising these two renal masses accurately. Sun et al. [45] reported that signal intensity changes of the corticomedullary phase on DCE MRI were the most effective parameter for distinguishing cc-RCC and p-RCC. Mysyck et al. [46] demonstrated that cc-RCC had the largest mean ADC value among the three subtypes, while ch-RCC had the lowest ADC value. Nevertheless, no report has compared the CS-SII values among the three subtypes. Our analysis of RCC subtypes also showed significantly different CS-SII values between cc-RCC and p-RCC (9.99 ± 1.44 vs -5.69 ± 1.38 , $p < 0.001$), and between cc-RCC and ch-RCC (9.99 ± 1.44 vs 1.82 ± 3.83 , $p < 0.05$) (Fig. 4), i.e. CS-SII measurements might aid the differentiation of cc-RCC from the other two major RCC subtypes.

Under electron microscopy, cc-RCC contains substantially more intracytoplasmic lipids than other histological RCC subtypes [9], yet only moderate amounts of intratumoural lipids (limited to that in the clear cell component) have been shown in p-RCC, and only small amounts have been shown in ch-RCC [9], which characterise the distinct SI values on opposed-phase MR images [3, 16, 47]. In their 2014 study, Childs et al. [48] found that visual in-phase SI loss occurred in 42% of p-RCC. In our study, p-RCC had negative CS-SII values, suggesting the presence of areas exhibiting increased SI on opposed-phase images in p-RCC. This might be helpful for identifying hemosiderin in p-RCC [49]. Moreover, the negative CS-SII value of p-RCC may be the reason for the decreased RCC CS-SII value, rendering the CS-SII values of mfAML and RCC indistinguishable (13.63 ± 1.77 vs 7.92 ± 1.61 , $p < 0.05$) (Fig. 4). Nevertheless, the difference between the p-RCC and ch-RCC CS-SII values was not significant ($p = 0.06$). Current multiparametric MRI, such as DCE and DWI,

Fig. 3 Forest plots of CS-SII values for cc-RCC (a), p-RCC (b), and ch-RCC (c)



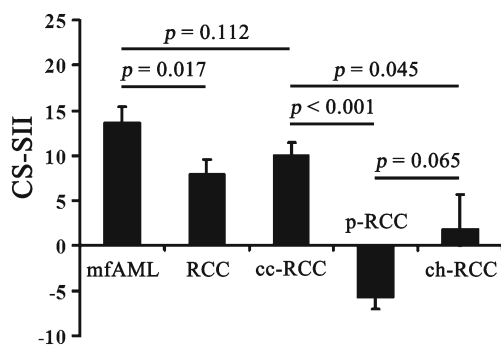


Fig. 4 Box and whisker plot of CS-SII values of mfAML, overall RCC, and the three main RCC subtypes. * $p < 0.05$, ** $p < 0.01$, *** $p < 0.001$

might be a valid diagnostic approach for accurate characterisation of these two renal masses.

Our meta-analysis has several limitations. First, as renal tumours are generally non-homogeneous, the various definitions of the ROIs and their reproducibility among different readers and papers (Table 1) may lead to different results in the literature on the value of CS-SII. Second, the number of included studies is relatively small, and to some extent the pooled results might be affected by inherent factors such as random error. Third, the CS-MRI series and field-strength parameters lack consensus, which would have influenced the CS-SII measurements. Furthermore, owing to the limitations of the published data (e.g. unavailability of individual patient data) and to heterogeneity, it was not possible to calculate the receiver operating characteristic (ROC) curves or a reliable threshold value. Fourth, publication bias is unavoidable for clinical evidence, as the relevant data were extracted from non-randomised controlled trials. Finally, as we excluded reports in languages other than English, there might have been language bias.

In summary, we conclude that the CS-SII values of CS-MRI cannot be used to accurately distinguish mfAML from cc-RCC, but cc-RCC has significantly higher CS-SII values than p-RCC and ch-RCC. Further adequately designed prospective studies with CS-MRI standardisation, especially standardisation of the cut-off threshold value, should be conducted to confirm our results.

Funding This study has received funding by the National Natural Science Foundation of China (81471705).

Compliance with ethical standards

Guarantor The scientific guarantor of this publication is Zhong-Qiu Wang, MD, PhD, (Department of Radiology, Affiliated Hospital of Nanjing University of CM, Nanjing 210029, China).

Conflict of interest The authors of this manuscript declare no relationships with any companies, whose products or services may be related to the subject matter of the article.

Statistics and biometry Pin Wang, PhD, (Department of Endocrinology, Sichuan Academy of Medical Science and Sichuan Provincial People's Hospital, Chengdu, Sichuan, China) kindly provided statistical advice for this manuscript.

Ethical approval Institutional Review Board approval was not required because we only performed data analysis based on the published studies.

Informed consent Informed consent was not required because this is a meta-analysis of several published papers and therefore data of our cohorts have been published already in these papers.

Methodology

- Diagnostic or prognostic study
- Performed at one institution

References

1. Bissler JJ, Kingswood JC (2004) Renal angiomyolipomata. *Kidney Int* 66:924–934
2. Bosniak MA, Megibow AJ, Hulnick DH et al (1988) CT diagnosis of renal angiomyolipoma: the importance of detecting small amounts of fat. *AJR Am J Roentgenol* 151:497–501
3. Catalano OA, Samir AE, Sahani DV et al (2008) Pixel distribution analysis: can it be used to distinguish clear cell carcinomas from angiomyolipomas with minimal fat? *Radiology* 247:738–746
4. Israel GM, Hindman N, Hecht E et al (2005) The use of opposed-phase chemical shift MRI in the diagnosis of renal angiomyolipomas. *AJR Am J Roentgenol* 184:1868–1872
5. Jinzaki M, Tanimoto A, Narimatsu Y et al (1997) Angiomyolipoma: imaging findings in lesions with minimal fat. *Radiology* 205:497–502
6. Thoenes W, Störkel S, Rumpelt HJ et al (1986) Histopathology and classification of renal cell tumors (adenomas, oncocytomas and carcinomas). The basic cytological and histopathological elements and their use for diagnostics. *Pathol Res Pract* 181:125–143
7. O'Toole KM, Brown M, Hoffmann P et al (1993) Pathology of benign and malignant kidney tumors. *Urol Clin North Am* 20:193–205
8. Hajdu SI, Savino A, Hajdu EO et al (1971) Cytologic diagnosis of renal cell carcinoma with the aid of fat stain. *Acta Cytol* 15:31–33
9. Krishnan B, Truong LD (2002) Renal epithelial neoplasms: the diagnostic implications of electron microscopic study in 55 cases. *Hum Pathol* 33:68–79
10. Hood MN, Ho VB, Smirniotopoulos JG et al (1999) Chemical shift: the artifact and clinical tool revisited. *Radiographics* 19:357–371
11. Namimoto T, Yamashita Y, Mitsuzaki K et al (2001) Adrenal masses: quantification of fat content with double-echo chemical shift in-phase and opposed-phase FLASH MR images for differentiation of adrenal adenomas. *Radiology* 218:642–646
12. Haider MA, Ghai S, Jhaveri K et al (2004) Chemical shift MR imaging of hyperattenuating (10 HU) adrenal masses: does it still have a role? *Radiology* 231:711–716
13. Hosokawa Y, Kinouchi T, Sawai Y et al (2002) Renal angiomyolipoma with minimal fat. *Int J Clin Oncol* 7:120–123
14. Delfaut EM, Beltran J, Johnson G et al (1999) Fat suppression in MR imaging: techniques and pitfalls. *Radiographics* 19:373–382
15. Karlo CA, Donati OF, Burger IA et al (2013) MR imaging of renal cortical tumours: qualitative and quantitative chemical shift imaging parameters. *Eur Radiol* 23:1738–1744

16. Outwater EK, Bhatia M, Siegelman ES et al (1997) Lipid in renal clear cell carcinoma: detection on opposed-phase gradient-echo MR images. *Radiology* 205:103–107
17. Peng XG, Ju S, Qin Y et al (2011) Quantification of liver fat in mice: comparing dual-echo Dixon imaging, chemical shift imaging, and ¹H-MR spectroscopy. *J Lipid Res* 52:1847–1855
18. Kim JK, Kim SH, Jang YJ et al (2006) Renal angiomyolipoma with minimal fat: differentiation from other neoplasms at double-echo chemical shift FLASH MR imaging. *Radiology* 239:174–180
19. Sasiwimonphan K, Takahashi N, Leibovich BC et al (2012) Small (<4 cm) renal mass: differentiation of angiomyolipoma without visible fat from renal cell carcinoma utilizing MR imaging. *Radiology* 263:160–168
20. Hindman N, Ngo L, Genega EM et al (2012) Angiomyolipoma with minimal fat: can it be differentiated from clear cell renal cell carcinoma by using standard MR techniques? *Radiology* 265:468–477
21. Ferré R, Cornelis F, Verkarre V et al (2015) Double-echo gradient chemical shift MR imaging fails to differentiate minimal fat renal angiomyolipomas from other homogeneous solid renal tumors. *Eur J Radiol* 84:360–365
22. Schieda N, Dilauro M, Moosavi B et al (2016) MRI evaluation of small (<4 cm) solid renal masses: multivariate modeling improves diagnostic accuracy for angiomyolipoma without visible fat compared to univariate analysis. *Eur Radiol* 26:2242–2251
23. Park JJ, Kim CK (2017) Small (<4 cm) renal tumors with predominantly low signal intensity on T2-weighted images: differentiation of minimal-fat angiomyolipoma from renal cell carcinoma. *AJR Am J Roentgenol* 208:124–130
24. Jhaveri KS, Elmi A, Hosseini-Nik H et al (2015) Predictive value of chemical-shift MRI in distinguishing clear cell renal cell carcinoma from non-clear cell renal cell carcinoma and minimal-fat angiomyolipoma. *AJR Am J Roentgenol* 205:W79–W86
25. Whiting PF, Rutjes AW, Westwood ME et al (2011) QUADAS-2: a revised tool for the quality assessment of diagnostic accuracy studies. *Ann Intern Med* 155:529–536
26. Hafron J, Fogarty JD, Hoenig DM et al (2005) Imaging characteristics of minimal fat renal angiomyolipoma with histologic correlations. *Urology* 66:1155–1159
27. Milner J, McNeil B, Alioto J et al (2006) Fat poor renal angiomyolipoma: patient, computerized tomography and histological findings. *J Urol* 176:905–909
28. Simpfendorfer C, Herts BR, Motta-Ramirez GA et al (2009) Angiomyolipoma with minimal fat on MDCT: can counts of negative-attenuation pixels aid diagnosis? *AJR Am J Roentgenol* 192:438–443
29. Roy C, Sauer B, Lindner V et al (2007) MR Imaging of papillary renal neoplasms: potential application for characterization of small renal masses. *Eur Radiol* 17:193–200
30. Pedrosa I, Sun MR, Spencer M et al (2008) MR imaging of renal masses: correlation with findings at surgery and pathologic analysis. *Radiographics* 28:985–1003
31. Kohl CA, Chivers FS, Lorans R et al (2014) Accuracy of chemical shift MR imaging in diagnosing indeterminate bone marrow lesions in the pelvis: review of a single institution's experience. *Skelet Radiol* 43:1079–1084
32. Wang X, Hemando D, Reeder SB et al (2016) Sensitivity of chemical shift-encoded fat quantification to calibration of fat MR spectrum. *Magn Reson Med* 75:845–851
33. Priola AM, Priola SM, Ciccone G et al (2015) Differentiation of rebound and lymphoid thymic hyperplasia from anterior mediastinal tumors with dual echo chemical-shift MR imaging in adulthood: reliability of the chemical shift ratio and signal intensity index. *Radiology* 274:238–249
34. Tsushima Y, Ishizaka H, Matsumoto M et al (2015) Adrenal masses: differentiation with chemical shift, fast low-angle shot MR imaging. *Radiology* 186:705–709
35. Fujiyoshi F, Nakajo M, Fukukura Y et al (2003) Characterization of adrenal tumors by chemical shift fast low-angle shot MR imaging: comparison of four methods of quantitative evaluation. *AJR Am J Roentgenol* 180:1649–1657
36. Reuter VE (2003) The pathology of renal epithelial neoplasms. *Semin Oncol* 33:534–543
37. Lim RS, Flood TA, McInnes MDF et al (2017) Renal angiomyolipoma without visible fat: Can we make the diagnosis using CT and MRI? *Eur Radiol*. <https://doi.org/10.1007/s00330-017-4988-4>
38. Kang SK, Huang WC, Pandharipande PV et al (2014) Solid renal masses: what the numbers tell us. *AJR Am J Roentgenol* 202:1196–1206
39. Amin MB, Amin MB, Tamboli P et al (2002) Prognostic impact of histologic subtyping of adult renal epithelial neoplasms: an experience of 405 cases. *Am J Surg Pathol* 26:281–291
40. Cheville JC, Lohse CM, Zincke H et al (2002) Comparisons of outcome and prognostic features among histologic subtypes of renal cell carcinoma. *Am J Surg Pathol* 27:612–624
41. Delahunt B, Bethwaite PB, Nacey JN (2007) Outcome prediction for renal cell carcinoma: evaluation of prognostic factors for tumours divided according to histological subtype. *Pathology* 39: 459–465
42. Escudier B, Eisen T, Stadler WM et al (2007) Sorafenib in advanced clear-cell renal-cell carcinoma. *N Engl J Med* 356:125–134
43. Motzer RJ, Hutson TE, Tomczak P et al (2007) Sunitinib versus interferon alfa in metastatic renal-cell carcinoma. *N Engl J Med* 356:115–124
44. Chowdhury S, Choueiri TK (2009) Recent advances in the systemic treatment of metastatic papillary renal cancer. *Expert Rev Anticancer Ther* 9:373–379
45. Sun MR, Ngo L, Genega EM et al (2009) Renal cell carcinoma: dynamic contrast-enhanced MR imaging for differentiation of tumor subtypes—correlation with pathologic findings. *Radiology* 250:793–802
46. Mytsyk Y, Dutka I, Borys Y et al (2016) Renal cell carcinoma: applicability of the apparent coefficient of the diffusion-weighted estimated by MRI for improving their differential diagnosis, histologic subtyping, and differentiation grade. *Int Urol Nephrol* 49: 215–224
47. Pedrosa I, Chou MT, Ngo L et al (2007) MR classification of renal masses with pathologic correlation. *Eur Radiol* 18:365–375
48. Childs DD, Clingan MJ, Zagoria RJ et al (2014) In-phase signal intensity loss in solid renal masses on dual-echo gradient-echo MRI: association with malignancy and pathologic classification. *AJR Am J Roentgenol* 203:W421–W428
49. Yoshimitsu K, Kakihara D, Irie H et al (2006) Papillary renal carcinoma: diagnostic approach by chemical shift gradient echo and echo-planar MR imaging. *J Magn Reson Imaging* 23:339–344